



Nanoscale
Horizons

**Simulated Annealing Fitting: A Global Optimization Method
for Quantitatively Analyzing Growth Kinetics of Colloidal Ag
Nanoparticles**

Journal:	<i>Nanoscale Horizons</i>
Manuscript ID	NH-COM-03-2021-000152.R1
Article Type:	Communication
Date Submitted by the Author:	28-Apr-2021
Complete List of Authors:	Wu, Siyu; Temple University, Department of Chemistry An, Qinwei; Temple University, Department of Chemistry Sun, Yugang; Temple University, Department of Chemistry

SCHOLARONE™
Manuscripts

COMMUNICATION

Simulated Annealing Fitting: A Global Optimization Method for Quantitatively Analyzing Growth Kinetics of Colloidal Ag Nanoparticles †

Received 00th January 20xx,
Accepted 00th January 20xx

Siyu Wu, Qinwei An and Yugang Sun *

DOI: 10.1039/x0xx00000x

The involvement of heterogeneous solid/liquid reaction in growing colloidal nanoparticles makes it challenging to quantitatively understand the fundamental steps that determine nanoparticles' growth kinetics. A global optimization protocol relying on simulated annealing fitting and LSW growth model is developed to analyze the evolution data of colloidal silver nanoparticles synthesized from a microwave-assisted polyol reduction reaction. Fitting all data points of the entire growth process determines with high fidelity the diffusion coefficient of precursor species and the heterogeneous reduction reaction rate parameters on growing silver nanoparticles, which represent the principal functions to determine the growth kinetics of colloidal nanoparticles. The availability of quantitative results is critical to understanding the fundamentals of heterogeneous solid/liquid reactions, such as identifying reactive species and reaction activation energy barriers.

We reported the measurement of growth kinetics of colloidal silver (Ag) nanoparticles in a microwave reactor using in situ high-energy x-ray diffraction (HEXRD), which was published in *Nano Letter* in 2016.¹ The availability of high-quality time-resolved HEXRD patterns offered the promise of quantifying the evolution kinetics of colloidal Ag nanoparticles in the course of reducing silver nitrate (AgNO₃) at elevated temperatures. The time-dependent mass evolution of the crystalline Ag nanoparticles exhibited sigmoidal shapes, and we mathematically fitted the data with a sigmoidal function, i.e., $y = a \left[1 - \frac{1}{1 + e^{\left(\frac{x-x_0}{dx}\right)}} \right]$. The data fitting determined the constant parameters of a , x_0 , and dx , which allowed us to conveniently compare the evolution kinetics under various reaction conditions (e.g., different temperatures and different

New Concepts: Real-time probing of colloidal nanoparticles' evolution kinetics in liquid solutions represents an emerging research area to understand the fundamental steps determining nanoparticle growth. The heterogeneous solid/liquid interfacial reactions responsible for growing nanoparticles in a closed system usually involve two primary interdependent functions, i.e., diffusion of reactive precursor species and surface reactions of the precursor species on the growing nanoparticles. Many attempts have been made to develop in situ techniques for measuring nanoparticle evolution. It is still challenging to quantitatively determine the intrinsic parameters (i.e., the diffusion coefficient of precursor and surface reaction rate constant) of the two intertwined functions. We apply the LSW model to describe the nanoparticle growth with an autonomous ordinary differential equation that is challenging to fit the in situ measurements of low/moderate-density data points. A new concept of global optimization protocol based on simulated annealing fitting is proposed to fit all data points of the entire growth process numerically. The fitting determine diffusion coefficients and surface reaction rate constants with high fidelity. The availability of intrinsic parameters' values offers the unprecedented opportunity to quantitatively understand the heterogeneous solid/liquid interfacial reactions of growing nanoparticles and rationally design the synthesis of colloidal nanoparticles.

concentrations of AgNO₃). However, the condition-dependent constants derived from the pure mathematic fitting were lack of physical meaning to represent the fundamental functions that determine the growth kinetics of colloidal nanoparticles. Professor Özkar and Professor Finke criticized this issue later in a paper published in *The Journal of Physical Chemistry C*,² in which they digitized our data and fitted the data with the Finke-Watzky (FW) two-step mechanism proposed by Professor Finke and Professor Watzky back to 1997.³ The FW two-step mechanism consists of slow, continuous nucleation with a reaction rate constant of k_1 and autocatalytic surface growth with a reaction rate constant of k_2 . The mechanism is generally

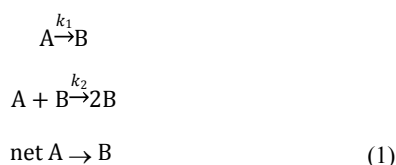
Department of Chemistry, Temple University, 1901 North 13th Street, Philadelphia, Pennsylvania 19122, United States

E-mail: ygsun@temple.edu

S.W. and Q.A. made equal contributions.

†Electronic Supplementary Information (ESI) available: Experiment details on the in situ experiment; Full-version LSW model describing the growth kinetics of colloidal Ag nanoparticles; Data processing and simulated annealing fitting of in situ experimental data; Density functional theory calculations on Ag-PVP complexes. See DOI: 10.1039/x0xx00000x

described in the format of serial (homogeneous) reactions as eq. 1:



where A and B stand for the precursor species and the composition species of the synthesized nanoparticles, respectively. Specifically, A represents Ag^+ ions and B represents Ag atoms of the growing Ag_n^0 nanoparticles in the aforementioned microwave-assisted synthesis of colloidal Ag nanoparticles. The rate law of the two-step reactions gives the time-dependent concentration of B, $[B]_t$, as a function of time, t , following

$$[B]_t = [A]_0 \left[1 - \frac{k_1 + k_2[A]_0}{k_2[A]_0 + k_1 e^{(k_1 + k_2[A]_0)t}} \right] \quad (2)$$

in which $[A]_0$ is the initial concentration of A. Eq. (2) provides a sigmoidal function to fit the data published in our 2016 *Nano Letters* paper. The fitting exercise determines the values of k_1 and k_2 with the fitting coefficient of determination (R^2) higher than 0.999, indicating the high quality of data fitting. We respectfully appreciate Professor Özkar and Professor Finke for their fitting efforts, and we do not comment on the suitability of FW two-step mechanism in describing the heterogeneous solid/liquid interfacial reactions involved in colloidal nanoparticle synthesis. The experimental HEXRD data reported in our 2016 *Nano Letters* paper primarily represent the growth kinetics of stable Ag nanoparticles because the nucleation process forms Ag nuclei that are too small (usually less than 2 nm) to give HEXRD signals. Therefore, we focus on analyzing growth kinetics of colloidal Ag nanoparticles assuming that the nucleation process has ceased to produce new nuclei when decent HEXRD patterns started to be observed.

The models reported in literature (including FW two-step mechanism) describe the growth of colloidal nanoparticles as autocatalytic surface reactions.²⁻⁶ Therefore, we believe that the mathematical equations describing the growth kinetics of colloidal nanoparticles should include the parameter of surface area (equivalent to r^2) of the growing nanoparticles. For example, the model proposed by Lifshitz, Slyozov, and Wagner (LSW model) is well known to describe the growth of colloidal particles after nucleation.^{5, 6} In such a multiple-phase system, growing solid particles dispersed in a liquid solution containing precursor species depends on two consecutive processes, i.e., the diffusion of precursor species to the surface of growing particles and the reaction of precursor species on the particles' surface (Figure 1a).^{7, 8} When one of the two processes plays the decisive role in the growth kinetics of colloidal nanoparticles, the LSW model can be simplified to an asymptotic format, i.e., either surface reaction-limited model (Figure 1b) or diffusion-limited model (Figure 1d).^{6, 9} The asymptotic models enable the feasibility to fit the in situ kinetic data of growing colloidal nanoparticles under the well-controlled synthesis conditions,

leading to the determination of fundamental parameters such as the diffusion coefficient (D) of precursor species in the reaction solution and the reaction rate constant (k) of the precursor species on growing nanoparticles' surface.¹⁰⁻¹⁴ In most cases of colloidal nanoparticle synthesis, either the asymptotic model cannot accurately reflect the growth kinetics since both the diffusion of precursor species and surface reactions contribute comparably to determine the growth kinetics (Figure 1c).⁹ The full-version LSW model including the contributions of both diffusion and surface reaction has to be applied to fit the in situ measurement data to simultaneously determine D and k with acceptable fidelity. Because of the complexity of the kinetic equation, accurate determination of D and k from fitting the in situ data is still challenging.

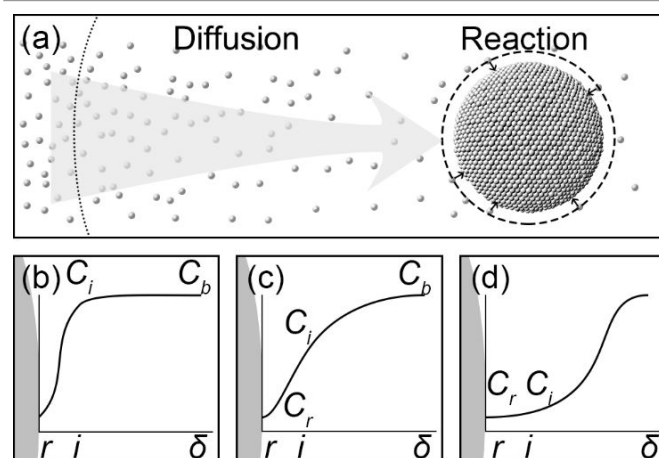


Figure 1. (a) Schematic illustration of the LSW model responsible for the growth of colloidal Ag nanoparticles, showing the diffusion of appropriate Ag(I) precursor species across the diffusion layer (dotted circle) followed by reduction of the Ag(I) precursor on the growing Ag nanoparticles in the interfacial layer (dashed circle). (b-d) Concentration gradient profiles for different LSW approximations: (b) surface reaction-limited model, (c) full LSW model, and (d) diffusion-limited model. The length scale in (a-d) does not represent the true values.

In this Communication, we report the use of simulated annealing (SA) fitting to analyze in situ data throughout the entire growth of colloidal nanoparticles using the full-version LSW model and determine the values of both D and k with high fidelity. We use in situ data of synthesizing Ag nanoparticles in microwave-assisted polyol reduction of AgNO_3 (reported in our 2016 *Nano Letters* paper; ESI[†], Section I) as an example to highlight the feasibility and accuracy of the SA fitting. In the synthesis, microwave heating was used to control the temperature of ethylene glycol (EG) solutions. Poly(vinyl pyrrolidone) (PVP) was added to serve as capping ligands to stabilize Ag nanoparticles. Successful determination of the values of fundamental kinetic parameters is promising to understand the thermodynamics and the active precursor species responsible for growing Ag nanoparticles. According to LSW model shown in Figure 1a (see ESI[†], Section II), the growth rate of the Ag nanoparticles is described as

$$\begin{cases} \frac{dr}{dt} = \frac{kD}{kr + D}(a - N_0 \cdot b \cdot r^3) \\ a = V_m \cdot C_0 \\ b = \frac{4\pi}{3V_s} \end{cases} \quad (3)$$

where r and t represent the radius of growing spherical Ag nanoparticles and the time, V_m , V_s , C_0 , and N_0 stand for molar volume of Ag metal ($10.3 \text{ cm}^3 \text{ mol}^{-1}$), the volume of reaction solution, initial concentration of AgNO_3 , and the number of growing Ag nanoparticles, respectively.

The autonomous ordinary differential equation (eq. 3) can be solved numerically using the classic fourth-order Runge-Kutta method (RK4)¹⁵ to give the nanoparticle growth trajectory $r(t)$ when the values of k and D are available, and an initial condition $r(t_0)$ is provided. On the other hand, when the nanoparticle growth trajectory $r(t)$ can be measured from in situ experiments, the values of k and D can be, in principle, determined by fitting the $r(t) \sim t$ data with eq. 3. In our 2016 paper the nanoparticle growth trajectory can be obtained from the total volume of Ag nanoparticles (V_{tot}), where $V_{\text{tot}} = \frac{4}{3}\pi r^3 N_0$ (see ESI[†], Section II, Figure S2c). The average size of the as-synthesized Ag nanoparticles (r_{max}) after the complete reduction of AgNO_3 was determined using transmission electron microscopy (TEM) imaging. The complete reduction of AgNO_3 generated the maximum total volume of Ag nanoparticles ($V_{\text{tot}}^{\text{max}}$) that was calculated from the amount of AgNO_3 added to the reaction solution. The number of growing Ag nanoparticles (N_0) could be calculated accordingly. The values of a and b were defined for a given reaction system. Fitting eq. 3 to the experimental data is reduced to a three-parameter estimation problem about k , D , and $r(t_0)$. To avoid the uncertainty of the initial condition $r(t_0)$ that is close to zero, we applied the two-way RK4 method that the initial condition $r(t_0)$ was set to the midpoint of the growth curve where the first derivative (i.e., dV_{tot}/dt) reaches the maximum. Since the size at the midpoint $r(t_{\text{mid}})$ of stable growing nanoparticles is a fixed non-zero number in a given synthesis, the actual freedom of the numerical fitting becomes two. We have developed an extreme-condition model to determine k and D using the simplified asymptotic LSW models by focusing on the growth at the very early stage (reaction-limited model) and the very late stage (diffusion-limited model).¹⁶ Because of the low density and small variation of experimental data points at the very early and the very late growth stages, the fidelity and accuracy of the fitted (k, D) values may be questionable. However, they can be used as the references as well as the initial guess for SA fitting to fit more experimental data points throughout the entire growth process, leading to improved fitting efficiency and saving computational time.

Since both k and D influence the growth rate of Ag nanoparticles, many different pairs of (k, D) can generate similar growth rate according to eq. 3 during the focused time periods, which results in a challenge to simultaneously determine the values of k and D with high fidelity from data fitting. We report the development of a global optimizing fitting protocol that allows fitting all data points of the entire growth process to minimize the possible errors. Specifically, a SA method¹⁷ allows a random search of the mathematically valid (k, D) pairs to determine the physically accurate (k, D) pair through statistical analysis. A C-program based on the SA algorithm is developed

to determine the optimum (k, D) pairs that give the least sum of squared residuals (SSR) of V_{tot} between the theoretical fitting predictions (V_{fit}) and experimental curve (V_{exp}) at each data point measured at different time t_i (see ESI[†], Section III):

$$SSR = \sum_i |V_{\text{fit}}(t_i) - V_{\text{exp}}(t_i)|^2 \quad (4)$$

At the beginning of the algorithm, a random (k, D) pair is chosen as the starting point. The program will jump randomly to a new (k, D) pair in a neighboring region and check whether the SSR of the new iteration ($n+1$) becomes smaller than the available record to give a better fitting to the experimental data. Possibility of acceptance (P) of the new (k, D) pair relies on the Metropolis jumping rule.¹⁸ A smaller SSR will be accepted immediately ($P=1$), and a larger SSR will be accepted with condition:

$$P(k, D) = \begin{cases} 1, & SSR_{n+1} < SSR \\ \exp\left(-\frac{|SSR_{n+1} - SSR|}{R\tau}\right), & SSR_{n+1} \geq SSR \end{cases} \quad (5)$$

in which R is a constant that is only related to the efficiency of the algorithm, τ is the current "temperature" of the SA process in analogy to metallurgical process. The value of τ decreases after each iteration of search, and the neighboring region for picking a new (k, D) pair narrows accordingly. A continuous search leads to a convergence of the (k, D) trace in the k - D plane to the point that possibly has the smallest SSR . Due to the Monte-Carlo feature (i.e., randomness and probability) of the SA algorithm, the best fitting result becomes more likely to reach as the program runs for enough time and iteration circles. In practice, the program is forced to stop when a set of criteria are fulfilled (e.g., the "temperature" of annealing lower than τ_{min}), avoiding the possible overfitting and saving the data processing time.

Figure 2(a) presents the (k, D) results from fitting the experimental data of growing Ag nanoparticles at $160 \text{ }^\circ\text{C}$ by repeating the SA program for 100 cycles. The (k, D) pair determined with the extreme-condition model was used as the starting point for the SA fitting. The likely optimized (k, D) pairs scatter around one of the branches of the rectangular hyperbola, i.e., $H = kD/(kr_i + D)$ with both r_i and H constants, in the k (horizontal) – D (vertical) plane. The (k, D) pairs with the smallest SSR s (red dots, Figure 2a) cluster in a confined region, highlighting the feasibility to determine the high-fidelity values of k and D . The distribution of k is very narrow (i.e., $2.5 \sim 3.1 \times 10^{-7} \text{ m}\cdot\text{s}^{-1}$) while the values of D scatter in a wider range (i.e., $5 \sim 10 \times 10^{-14} \text{ m}^2\cdot\text{s}^{-1}$), suggesting that k can be more accurately determined than D . Such difference indicates that the contribution of surface reaction to the growth kinetics of Ag nanoparticles at $160 \text{ }^\circ\text{C}$ is more determining than the contribution of precursor diffusion. Considering that the SA algorithm suggests the uncertainty of the fitting results, we use the averages of the top 10% results from the 100 circles of the SA fitting to improve the accuracy. The statistic accuracy of k evaluated from the clustered (k, D) pairs with the smallest SSR s is higher than that of D , i.e., $(2.87 \pm 0.052) \times 10^{-7} \text{ m}\cdot\text{s}^{-1}$ for k with statistic deviation of 18% versus $(8.13 \pm 2.24) \times 10^{-14} \text{ m}^2\cdot\text{s}^{-1}$ for D

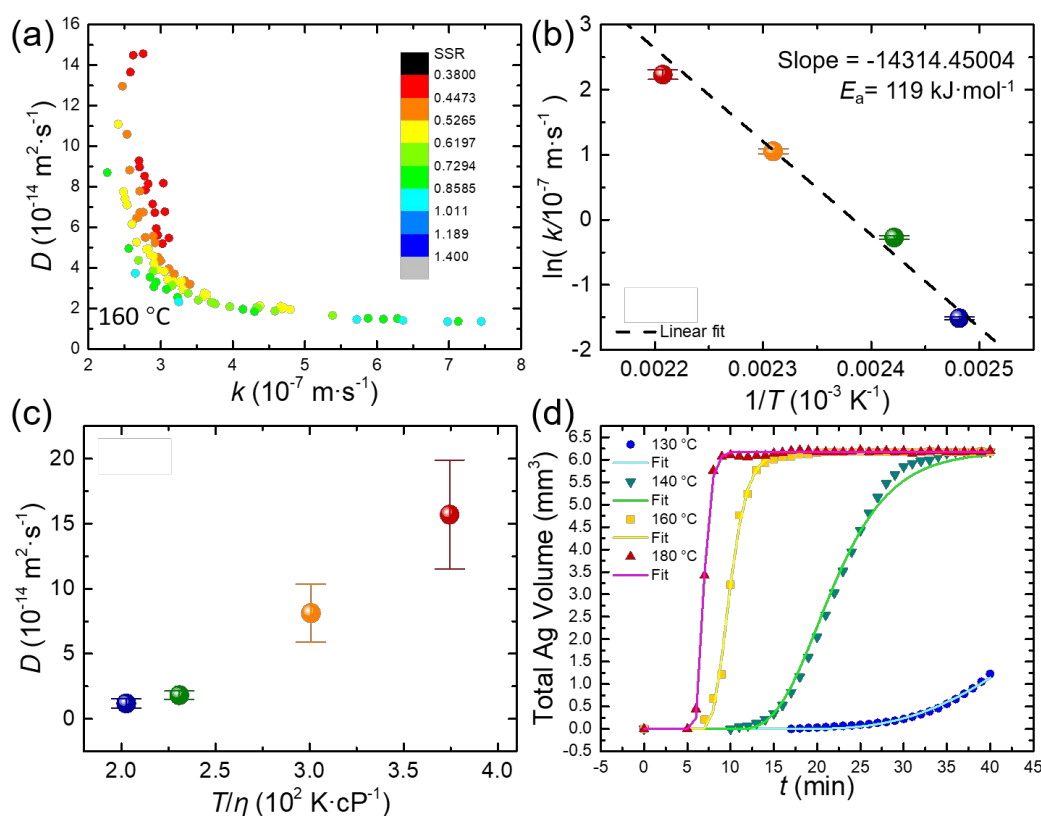


Figure 2. (a) The optimized (k , D) pairs determined from the SA fitting of the growth kinetics of colloidal Ag nanoparticles measured from the synthesis at 160 °C. The concentration of AgNO_3 was 0.1 M and the concentration of PVP in terms of repeat unit was 0.15 M. The colors of dots correspond to the SSRs calculated between the experimental data and the fitting data. (b) Plot of $\ln(k)$ as a function of $1/T$. (c) Dependence of D on T/η . (d) Plots of the fitted kinetic curve and the measured data (symbols) of the synthesis at different temperatures: 130 °C (blue, ●), 140 °C (green, ▼), 160 °C (yellow, ■), and 180 °C (red, ▲).

with statistic deviation of 28%. It is worthy of pointing out that the (k , D) pairs with the smallest SSRs derived from the SA fitting cluster at the upper arm of the half hyperbola to highlight the more reaction-limited growth of Ag nanoparticles. Such a conclusion is consistent with $k \cdot r_{\text{max}}/D < 1$, which is calculated using the fitted (k , D) values (see ESI†, Table S2).

The growth kinetics of Ag nanoparticles accelerates significantly with the reaction temperature. The SA fitting reveals that increasing temperature leads to the increase of both the diffusion of Ag(I) precursor and the surface reduction of Ag(I) precursor species on growing Ag nanoparticles. The values of k and D of the syntheses at varying temperatures, e.g., 130 °C, 140 °C, 160 °C, and 180 °C, are presented in Table S2 (see ESI†). When temperature increases from 130 °C to 180 °C, k increases by 42.4 times from $0.22 \times 10^{-7} \text{ m}\cdot\text{s}^{-1}$ to $9.33 \times 10^{-7} \text{ m}\cdot\text{s}^{-1}$. The logarithm of the temperature-dependent reaction rate constant (i.e., $\ln k$) exhibits a linear relationship with the reciprocal of thermodynamic temperature ($1/T$) (Figure 2b). According to the Arrhenius equation $k = Ae^{-E_a/RT}$ (R and A representing the universal gas constant and the frequency factor), the activation energy (E_a) of reducing the Ag(I) precursor on growing Ag nanoparticles in EG is calculated to be 119.0 $\text{kJ}\cdot\text{mol}^{-1}$.

The clustering center of the D values increases by 13.2 times from $1.19 \times 10^{-14} \text{ m}^2\cdot\text{s}^{-1}$ to $1.57 \times 10^{-13} \text{ m}^2\cdot\text{s}^{-1}$ as temperature increases from 130 °C to 180 °C (Figure 2c, Table S2, see ESI†). According to the Stokes-Einstein equation, $D = \frac{k_B \cdot T}{6\pi \cdot \eta \cdot r_{dy}}$ the

diffusion coefficient (D) of a dynamic spherical molecule is proportional to temperature (T) and inversely proportional to the viscosity (η) of the solvent and the dynamic radius of the diffusive molecule (r_{dy}). Figure 2c shows the dependence of D derived from the SA fitting on T/η , in which the temperature-dependent viscosity of a PVP-EG solution is adjusted according to the reported data.¹⁹ The plot is linear despite the first data point collected at 130 °C, where the growth curve is incomplete and may not represent the true D value. The accuracy of the values of k and D determined from the SA fitting can be evaluated by comparing the theoretical growth kinetics calculated from eq. (3) with the experimental growth kinetics. The good agreement is shown in Figure 2d, highlighting the high fidelity of the SA fitting in determining k and D .

The SA fitting is also applied to analyze the growth kinetics of colloidal Ag nanoparticles synthesized with different concentrations ($C_0 = 0.05 \text{ M}$, 0.10 M , and 0.15 M) of AgNO_3 at a constant temperature of 160 °C and a constant concentration of PVP (0.15 M) (Figure 3a). The values of k and D determined from these syntheses are presented in Table S3 (see ESI†). The diffusion coefficient of reactive precursor species, D , remains essentially constant around $\sim 10 \times 10^{-14} \text{ m}^2\cdot\text{s}^{-1}$ (Figure 3b), which is consistent with the Stokes-Einstein equation. In contrast, the fitted surface reaction rate constant, k , decreases from $6.21 \times 10^{-7} \text{ m}\cdot\text{s}^{-1}$ to $2.12 \times 10^{-7} \text{ m}\cdot\text{s}^{-1}$ as the concentration of AgNO_3 increases from 0.05 M to 0.15 M (Figure 3c). According to the Arrhenius equation, the surface reaction rate constant should not vary with the precursor concentration at a constant

temperature. The deviation of the fitted k and the expected k implies that the actual precursor involved in the surface reduction for growing Ag nanoparticles is not AgNO_3 (or Ag^+).

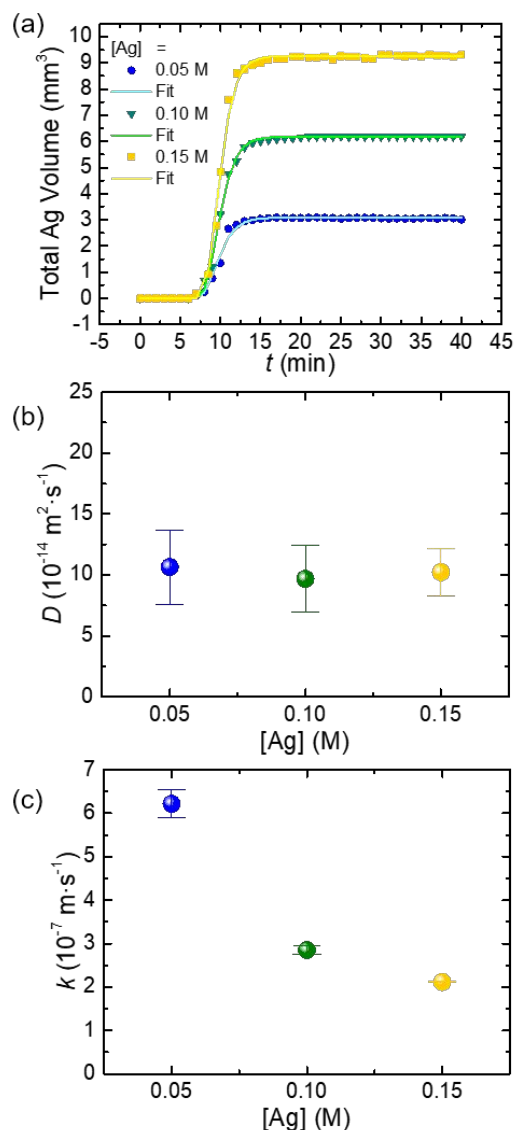


Figure 3. Analysis of time-resolved HEXRD patterns recorded in the growth of colloidal Ag nanoparticles at different AgNO_3 concentrations: 0.05 M (blue, ●), 0.10 M (green, ▼), and 0.15 M (yellow, ■). (a) Total Ag volume as a function of time (symbols) at different AgNO_3 concentrations and their corresponding theoretical calculation (curves) using the SA fitting. (b) Diffusion coefficient (D) at different AgNO_3 concentrations. (c) Reaction rate constant (k) at different AgNO_3 concentrations.

We have performed the basic density functional theory (DFT) calculations on the interactions between Ag^+ ions (or Ag^0 atoms) and vinylpyrrolidone (VP) repeat unit (see ESI[†], Section IV). The calculation results show that the linear coordination of Ag ions to the carbonyl groups of VP units is thermodynamically favorable (see ESI[†], Figure S7), which is consistent with claims proposed in the previous report.²⁰ The formation of Ag^+ -O-VP complex enriches the electron densities on the Ag^+ ions due to electron donation of the pyrrolidone ring, benefiting the reduction of Ag(I) to metallic Ag.²¹ Therefore, the actual

precursor species involved in the surface reaction is Ag^+ -O-VP complex rather than all Ag(I) species that is used in the SA fitting. According to the LSW model, the consumption rate of Ag(I) species due to the surface reaction on growing Ag nanoparticles is described as (eq. S2, see ESI[†]):

$$J_{\text{rxn}} = 4\pi r^2 k (C_i - C_r) \approx 4\pi r^2 k \cdot C_i \quad (6)$$

where C_i represents the concentration of Ag(I) precursor at the imagined solid/liquid interface i (the dashed circle in Figure 1a). C_r is the concentration of Ag(I) precursor near the surface of a Ag nanoparticle, which is equal to the negligibly low solubility of the Ag atoms under the reaction condition. For the growing Ag nanoparticles with a radius of r , $k_{\text{fit}} \cdot C_{i, \text{total Ag(I)}} = k_{\text{actual}} \cdot C_{i, \text{Ag}^+ - \text{O} - \text{VP}}$, in which k_{fit} is the rate constant (shown in Figure 3c) determined from the fitting process using the concentration of total Ag(I) in bulk solution, k_{actual} stands for the rate constant corresponding to the actual reaction precursor of Ag^+ -O-VP complex. This equation is rewritten as

$$\frac{C_{i, \text{Ag}^+ - \text{O} - \text{VP}}}{C_{i, \text{total Ag(I)}}} = \frac{k_{\text{fit}}}{k_{\text{actual}}} \quad (7)$$

The left term represents the fraction of Ag^+ coordinated with PVP. When the concentration of PVP is constant, a higher concentration of AgNO_3 gives a lower $\frac{C_{i, \text{Ag}^+ - \text{O} - \text{VP}}}{C_{i, \text{total Ag(I)}}}$ at constant temperature. Since the principle k_{actual} is constant at a given temperature, the value of k_{fit} determined from the SA fitting is smaller at a higher concentration of AgNO_3 , which is observed in Figure 3c.

Conclusions

In summary, a global fitting method based on SA algorithm has been developed to fit the experimentally measured growth kinetics of colloidal nanoparticles using the full-version LSW model. The fitting applies to all data points throughout the entire growth process determined by both surface reaction and diffusion of precursor species, resulting in the extraction of reliable k and D . According to the principle of the LSW model, the presented fitting protocol readily applies to the synthesis of colloidal nanoparticles, in which continuous growth of colloidal nanoparticles is supported by the surface reaction after burst nucleation. Availability of the fundamental kinetics parameters, k and D , is crucial to understand the insightful details of nanoparticle growth. For example, the precursor species involved in the surface reaction on growing Ag nanoparticles is determined, for the first time, as Ag^+ -O-VP complex. The activation energy of the surface reduction of Ag^+ -O-VP complex on the growing Ag nanoparticles is 119.0 kJ·mol⁻¹. The global fitting and quantitative understanding of growth kinetics of colloidal nanoparticles provide a promising strategy for understanding the in-depth mechanism of surface reactions on growing nanoparticles.

Conflicts of interest

There are no conflicts to declare.

Acknowledgements

This work was supported by the National Science Foundation under NSF award 1946912. We thank Prof. Spiridoula Matsika on the tutoring and guidance on the DFT calculations.

References

- 1 Q. Liu, M. R. Gao, Y. Liu, J. S. Okasinski, Y. Ren and Y. Sun, *Nano Lett.*, 2016, **16**, 715-720.
- 2 S. Özkar, and R. G. Finke, *J. Phys. Chem. C*, 2017, **121**, 27643-27654.
- 3 M. A. Watzky and R. G. Finke, *J. Am. Chem. Soc.*, 1997, **119**, 10382-10400.
- 4 J. D. Martin, *Chem. Mater.*, 2020, **32**, 3651-3656.
- 5 I. M. Lifshitz, and V. V. Slyozov, *J. Phys. Chem. Solids*, 1961, **19**, 35-50.
- 6 C. Wagner, *Ber. Bunsen-Ges. Phys. Chem.*, 1961, **65**, 581-591.
- 7 T. Sugimoto, *Monodispersed Particles*. Elsevier: Amsterdam, NL, 2001.
- 8 N. T. Thanh, N. Maclean, and S. Mahiddine, *Chem. Rev.*, 2014, **114**, 7610-7630.
- 9 R. Viswanatha, P. K. Santra, C. Dasgupta, and D. D. Sarma, *Phys. Rev. Lett.*, 2007, **98**, 255501.
- 10 H. Zheng, R. K. Smith, Y. W. Jun, C. Kisielowski, U. Dahmen, and A. P. Alivisatos, *Science*, 2009, **324**, 1309-1312.
- 11 J. M. Yuk, J. Park, P. Ercius, K. Kim, D. J. Hellebusch, M. F. Crommie, J. Y. Lee, A. Zettl, and A. P. Alivisatos, *Science*, 2012, **336**, 61-64.
- 12 J. Lee, J. Yang, S. G. Kwon, and T. Hyeon, *Nat. Rev. Mater.*, 2016, **1**, 16034.
- 13 H. G. Liao, D. Zherebetsky, H. Xin, C. Czarnik, P. Ercius, H. Elmlund, M. Pan, L. W. Wang, and H. Zheng, *Science*, 2014, **345**, 916-919.
- 14 Y. Sun, X. Zuo, S. Sankaranarayanan, S. Peng, B. Narayanan, and G. Kamath, *Science*, 2017, **356**, 303-307.
- 15 C. Runge, *Math. Ann.*, 1895, **46**, 167-178.
- 16 S. Wu, and Y. Sun, *Nano Res.*, 2019, **12**, 1339-1345.
- 17 T. J. P. Penna, *Comput. Phys.*, 1995, **9**, 341-343.
- 18 B. Gidas, in *Topics in Contemporary Probability and Its Applications*, ed. J. L. Snell, CRC, Boca Raton, FL, 1995, ch. 7, 159-232.
- 19 W. Yu, H. Xie, L. Chen, and Y. Li, *Powder Technol.*, 2010, **197**, 218-221.
- 20 X. Xia, J. Zeng, L. K. Oetjen, Q. Li, and Y. Xia, *J. Am. Chem. Soc.*, 2012, **134**, 1793-1801.
- 21 C. Wu, B. P. Mosher, K. Lyons, and T. Zeng, *J. Nanosci. Nanotechnol.*, 2010, **10**, 2342-2347.